NANO LETTERS

pubs.acs.org/NanoLett Letter

DNA-Modified Plasmonic Sensor for the Direct Detection of Virus Biomarkers from the Blood

Abraham Vázquez-Guardado, Freya Mehta, Beatriz Jimenez, Aritra Biswas, Keval Ray, Aliyah Baksh, Sang Lee, Nileshi Saraf, Sudipta Seal, and Debashis Chanda*

Cite This: https://doi.org/10.1021/acs.nanolett.1c01609 Read Online

ACCESS | Metrics & More | Article Recommendations | Supporting Information

ABSTRACT: The rapid spread of viral infections demands early detection strategies to minimize proliferation of the disease. Here, we demonstrate a plasmonic biosensor to detect Dengue virus, which was chosen as a model, via its nonstructural protein NS1 biomarker. The sensor is functionalized with a synthetic single-stranded DNA oligonucleotide and provides high affinity toward NS1 protein present in the virus genome. We demonstrate the detection of NS1 protein at a concentration of 0.1−10 μg/mL in bovine blood using an on-chip microfluidic plasma separator integrated with the plasmonic sensor which covers the clinical threshold of 0.6 μg/mL of high risk of developing Dengue hemorrhagic fever. The conceptual and practical demonstration shows the translation feasibility of these microfluidic optical biosensors for early detection of a wide range of viral infections, providing a rapid clinical diagnosis of infectious diseases directly from minimally processed biological samples at point of care locations.

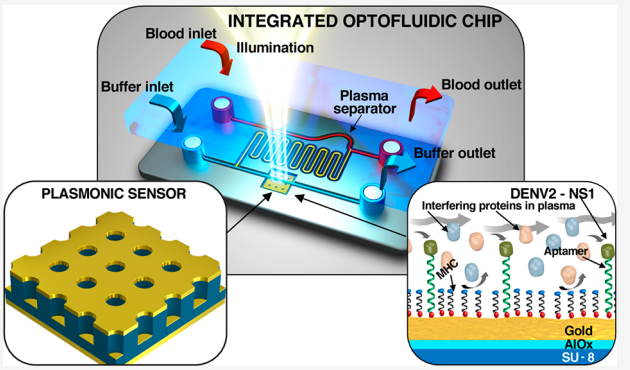

KEYWORDS: *Biosensing, viral infections, plasmonics, nanoimprinting, microfluidic systems*

Viral infections are one of the topmost health concerns worldwide, especially those highly contagious that emerge from isolated geographical clusters and evolve rapidly into pandemics.[1,2] For instance, Dengue virus (DENV), a member of the *Flaviviridae* family and transmitted by female mosquitoes (*Aedes aegypti* or *Aedes albopictus*), produces a spectrum of clinical illnesses ranging from acute Dengue fever (DF), to deadly hemorrhagic fever (DHF), or the Dengue shock syndrome (DSS).[2−4] The four DENV serotypes (DENV1, DENV2, DENV3, and DENV4) are a prevailing threat to almost half of the world's population especially those at tropical latitudes where viral vectors are abundant.[2] In fact, it is estimated that 50 million DENV infections occur around the world each year and approximately 1% of these infections will require hospitalization as they develop into DHF or DSS.[2] Currently, there is no specific treatment for DENV infections, partly because the pathogenesis is not clearly understood.[5−7] Furthermore, efforts to develop and deploy an effective vaccine against all DENV serotypes have remained elusive, and the current approved vaccine (CYT-TVDV, Sanofi Pasteur) still has below 60% efficacy against the four DENV serotypes in children 2−17 years old.[8,9] Thus, the early detection followed by aggressive clinical intervention remains as one of the best ways to manage the infection and prevent chronic pathologies or death, and at the same time it becomes a strategic measure to contain the spread.[1,2]

Viral infections, such as DENV, are diagnosed using antibody, protein biomarkers, or messenger ribonucleic acid (mRNA) from a biological sample. On one hand, the enzyme-linked immunosorbent assay (ELISA) is the clinical diagnostic gold standard for seral antibodies or proteins detection, which is an indirect approach to identify an active or past viral infection.[10,11] On the other hand, the reverse transcriptase polymerase chain reaction (RT-PCR) specifically targets viral mRNA strands with high accuracy, which is ideal for the diagnosis of active viral infections with specific genome specificity.[12,13] However, the cost of the time-consuming process, the dedicated infrastructure, and the extensive sample preparation in both cases restrict the proliferation beyond commercial laboratories and academic environments. Alternative label-free affinity biosensors promise to develop assays for the rapid diagnosis of pathogenetic biomarkers, for example, those based on localized surface plasmon (LSP).[14,15] These devices are extremely sensitive when

Received: April 23, 2021
Revised: August 12, 2021

https://doi.org/10.1021/acs.nanolett.1c01609
Nano Lett. XXXX, XXX, XXX−XXX

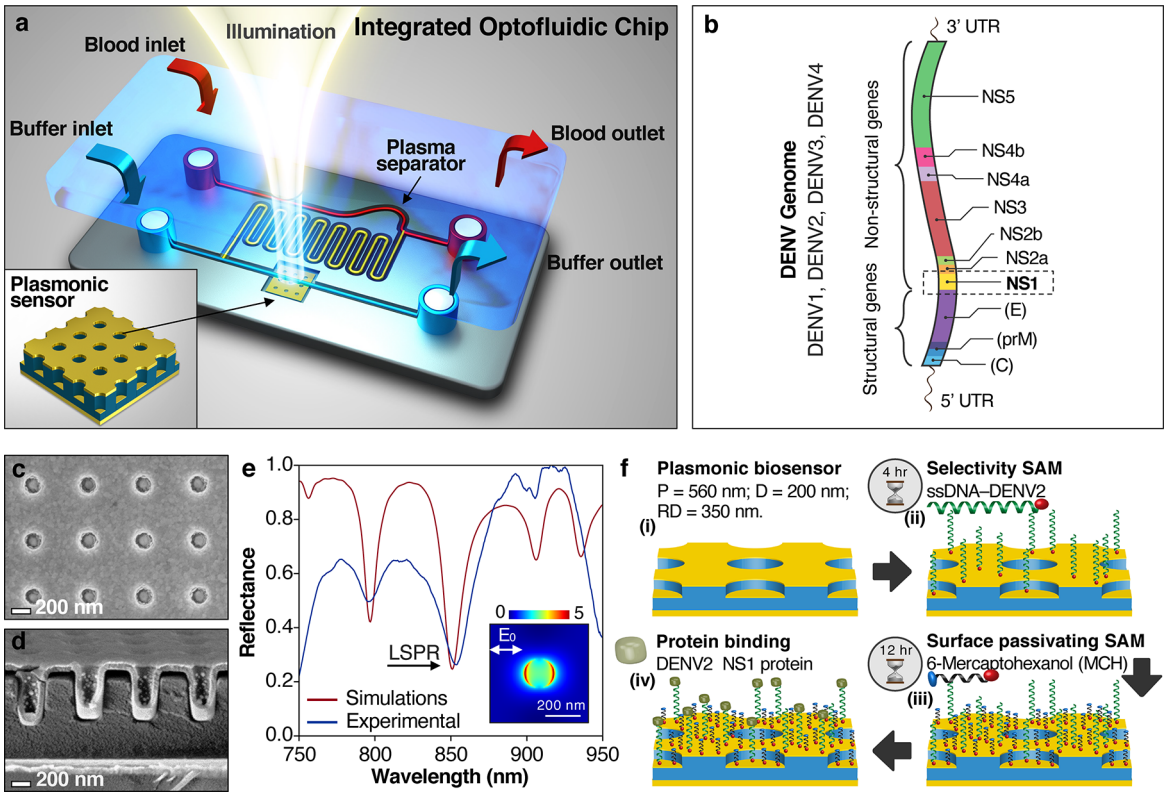

Figure 1. (a) Integrated Dengue virus biosensor comprising an in-line microfluidic blood plasma separator and a cavity-coupled nanoimprinted plasmonic array. Inset corresponds to the nanoimprinted plasmonic biosensor composed of a gold mirror (80 nm), a dielectric film spacer (~700 nm) embossed with a square array of holes, a conformal thin film of aluminum oxide layer (20 nm) as fluid barrier, and a thin gold film (30 nm). (b) Dengue virus genome shared among the four DENV serotypes and comprised of three structural (C, prM, and E) and seven nonstructural (NS) proteins, including NS1. (c,d) Scanning electron microscope images, top view (c) and cross section (d), of one representative nanoimprinted sensor. (e) Reflectance spectra obtained using FDTD simulations (red curve) and experimentally (blue curve). Inset represents the electric field enhancement obtained 5 nm above the circular hole at the LSPR. (f) Representation of the biosensing workflow. (i) The sensors are batch prepared and properly cleaned prior to functionalization. (ii) Thiol-terminated ssDNA aptamer specific to nonstructural DENV2-NS1 protein binds covalently to the gold surface. This step requires incubation for 4 h. (iii) Thiol-terminated 6-mercaptohexanol (MCH) self-assembly monolayer binds covalently to the empty surface area to block nonspecific binding and decrease protein fouling present in biological fluids. This process requires incubation for 12 h. (iv) DENV2-NS1 protein detection via aptamer binding, which produces a readable LSPR shift.

properly functionalized reaching detection of biomolecules in the pico- to femtomolar concentrations.

In this work, we demonstrate a cavity-coupled plasmonic biosensor integrated with a microfluidic blood plasma separator[16−18] to detect the DENV biomarker directly from blood as schematically shown in Figure 1a. The cavity coupling improves the quality factor Q (bandwidth, $\Delta\lambda$) of the LSP resonance while large area parallel nanoimprinting-based patterning ensures deterministic resonance replication (λ_R).[16,19] In order to make it target specific, the plasmonic biosensor is functionalized with a high-affinity single stranded DNA (ssDNA) aptamer against the nonstructural NS1 protein from DENV2 serotype, Figure 1b. In addition, we implemented a surface passivation scheme based on thiol-terminated 6-mercaptohexanol (MCH) self-assembled monolayer to minimize nonselective binding from proteins present in biological fluids, such as blood plasma. With such surface functionalization and passivation strategy in conjunction with an antiswelling protective layer, we demonstrate the detection of NS1 protein from DENV2 at a concentration of 0.1−10 μg/mL in bovine blood using a plasma separating microfluidic chip integrated with this plasmonic biosensor. This concentration range covers the clinical threshold of 0.6 μg/mL for predicting high risk of developing DHF in DENV infected patients.[11,20]

The plasmonic sensor used in this work is formed by hybridizing the LSP resonance (LSPR) with an asymmetric Fabry−Perot cavity resonator.[17,19,21] The plasmonic nanostructure, unlike conventional one metallic element, is composed of two complementary elements, hole/disk, of period/diameter of 560/200 nm and separated by 350 nm relief depth. The pattern is thermally embossed on UV curable epoxy SU-8 and coated with 30 nm of gold, see Figure 1a (inset). Further, the complementary hole/disk array is far-field coupled with the photonic cavity formed by an optically thick (100 nm) gold back reflector separated from the plasmonic nanostructure by a thick SU-8 spacer film (typically 700 nm). Applications where the plasmonic device is submerged in solvents, including water, for prolonged periods of time leads to SU-8 swelling,[22] which could add finite cavity thickness variations observed in spurious LSPR shift. In order to prevent this detrimental effect, a conformal antiswelling 20 nm aluminum oxide membrane is grown on the polymeric nanohole array prior to metal evaporation to prevent water diffusion into the epoxy matrix, see Methods in the Supporting Information for details. Figure 1a (inset) depicts the schematic representation of this system, and the corresponding scanning electron microscope (SEM) image of one representative device with cavity thickness of ~700 nm is shown in Figure 1c,d.

https://doi.org/10.1021/acs.nanolett.1c01609
Nano Lett. XXXX, XXX, XXX−XXX

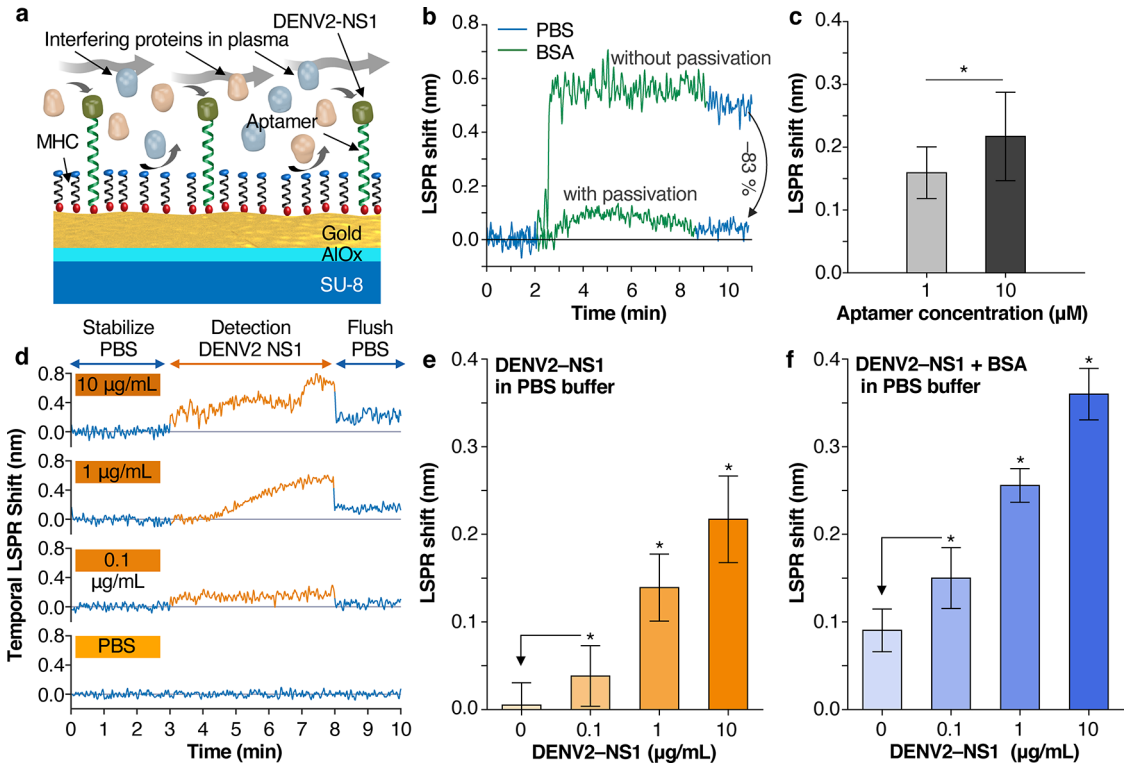

Figure 2. (a) Biosensing representation from biological fluid. The surface passivation strategy decreases protein fouling while permitting the binding of the biomarker to the ssDNA aptamer. (b) Demonstration of thiol-terminated 6-mercaptohexanol (MCH) surface passivation against BSA adsorption (100 μg/mL in PBS). The surface passivated sensor reduces up to 83% of the sensor residual response with respect to its nonpassivated counterpart. (c) Biosensing demonstration with simultaneous passivation and functionalization. The sensors are functionalized with two aptamer concentrations (1 and 10 μM) tested with same 10 μg/mL DENV2-NS1 concentration in PBS. (d) LSPR time evolution for three DENV2-NS1 protein concentrations (0.1, 1, and 10 μg/mL) in PBS and one control (only PBS, or zero concentration). Sensorgrams are color-coded to show the time stamps at which the flow events were happening. (e) LSPR shift quantization of the four sensorgrams shown in (d) as a function of DENV2-NS1 protein concentration. (f) LSPR shift quantization of three DENV2-NS1 protein concentration in PBS solution with additional 100 μg/mL BSA concentration and control sample (only PBS+BSA, or zero concentration). Error bars are the standard deviation from the mean. *Unpaired t test and one-way ANOVA with Tukey pairwise comparison ($p < 0.001$).

Cavity-coupled plasmonic systems support hybridized LSP oscillation modes in the top metallic nanostructure that, when coupled with a back metallic reflector, form an asymmetric photonic cavity. Figure 1e shows the reflection spectra obtained using finite difference time domain (FDTD) simulations (Q factor of 53) compared with that obtained experimentally (Q factor of 37) when immersed in aqueous solution (n = 1.333), see Methods in the Supporting Information for details. At resonance (LSPR ~ 850 nm) the hole/disk array supports a plasmonic resonance (inset in Figure 1e) which is extremely sensitive to changes in the surrounding medium, resulting in a measurable shift in the resonance frequency.

Nonstructural NS1 glycoprotein forms part of the genetic code of all the *Flaviviridae* virus family, such as the four serotypes of the DENV, the Japanese encephalitis virus, Yellow fever virus, West Nile virus, tick-borne Encephalitis virus, and Zika virus.[23−25] Figure 1b shows the DENV genome which is not different from the general *Flaviviridae* virus family.[25] However, such a genomic similarity does not translate to a genetic material homogeneity. For example, only 23% of the protein genome is conserved among these virus genera. In addition, DENV2 shares 71.44% with DENV1, 71.64% with DENV3, 68.82% with DENV4, 55.44% with Zika virus, 51.96% with West Nile virus, and 45.46% with Yellow fever virus.[25,26] NS1 proteins, a constituent of the DENV genome, plays an important role in the virus replication process and is secreted into the bloodstream by the infected cells, thus it becomes a representative biomarker for the identification of the infection.[27,28] It was demonstrated that high levels in acute-phase serum samples correlated with high risk of developing DHF.[11,20] Hence, detection directly from the blood, or plasma, is essential in order to avoid fatalities.

The sensor is functionalized with ssDNA aptamer to detect NS1 protein directly from blood. However, detection from minimally processed and unfiltered biological samples in general is challenging due to the protein adsorption on sensor surface. The high protein content in blood plasma tends to electrostatically accumulate on the negatively charged gold surface producing spurious biofilm accumulation leading to uncontrolled background masking the positive binding of the target biomarker. In order to address such a protein fouling, we implement surface passivation based on thiol-terminated 6-mercaptohexanol (MCH) self-assembled monolayer, which is a typical surface passivating strategy for gold-based biosensors.[29−31] The functionalization and biosensing workflow are graphically represented in Figure 1f. The plasmonic substrates were batch nanoimprinted (Figure 1f-i), functionalized with commercially available thiol-terminated ssDNA aptamer against the NS1 protein from DENV2 (DENV2-NS1) serotype (Base Pair Biotechnologies Inc.) (Figure 1f-ii), followed by surface MCH passivation (Figure 1f-iii), and finally NS1

https://doi.org/10.1021/acs.nanolett.1c01609
Nano Lett. XXXX, XXX, XXX−XXX

protein binding detection using optical reflection spectroscopy and subsequent quantization by LSPR shift (Figure 1f-iv), see Methods in the Supporting Information for details.

This specialized surface functionalization and passivation enables detection of the target antigen even in the presence of high protein content in the biological sample, as can be seen in Figure 2a. The sensor passivation was characterized first using 100 μg/mL bovine serum albumin (BSA) in phosphate buffer saline (PBS) as a model for nonspecific interfering protein contained in biological samples. Two nonfunctionalized plasmonic substrates were prepared with and without surface passivation. This PBS+BSA solution was delivered using a microfluidic chip placed on top of the plasmonic substrate and secured with an acrylic fixture, see Methods in the Supporting Information for details. First, PBS flows in the microfluidic channel to bring the sensor to a stable state determining the baseline. Then the PBS+BSA solution flows for 5 min and then is flushed away with PBS to remove poorly adhered BSA on the gold surface. Protein adsorption and selective binding in the subsequent biosensing demonstrations is gauged using the LSPR shift with respect to the baseline. In the plasmonic substrate without passivation, BSA accumulates rapidly within half a minute and remains constantly independent of the continuous BSA flow which is a sign of surface saturation. The flow of PBS solution flushes any poorly adhered BSA, but the residual LSPR shift (0.497 $\pm$ 0.028 nm) denotes a considerable remaining protein adhesion to the substrate, see Figure 2b. In contrast, BSA minimally affects the surface passivated substrate observed in the slower sensor response and the small residual LSPR shift (0.083 $\pm$ 0.018 nm) after PBS flush. This strategy achieves ~83% reduction in the residual LSPR shift. After confirming the surface passivation implementation, we tested the plasmonic biosensor with simultaneous ssDNA aptamer functionalization and surface passivation. Two sensors were functionalized with 1 and 10 μM ssDNA aptamer concentration and 10 μg/mL purified DENV2-NS1 protein in PBS buffer was flown in the same pattern as described in the previous surface passivation characterization. Figure 2c shows the LSPR shift, which confirms that the sensor binds the biomarker at two strengths commensurate with the surface coverage of the ssDNA aptamer; 10 μM ssDNA aptamer concentration was employed in all the subsequent biosensing demonstrations.

The first detection demonstration is performed in PBS solution where purified DENV2-NS1 protein was spiked at different known concentrations. The purpose of this characterization is to evaluate the binding capability to detect the target biomarker within the clinically relevant concentration for high risk DHF development (0.6 μg/mL).[11,20] A batch of sensors were fabricated, functionalized, and surface passivated, see Methods in the Supporting Information for details. Using the integrated microfluidics system, each sensor was exposed to different DENV2-NS1 protein concentrations, 0.1, 1, and 10 μg/mL, including a control solution (in this case just PBS). The sensors were first stabilized with PBS running buffer, then the PBS+DENV2-NS1 solution flowed for 5 min followed by PBS flush, while continuously collecting the reflection spectra at each second interval using a spectrometer automated with a customized LabVIEW (National Instruments) graphic user interface, see Methods in the Supporting Information for details. Typical time evolution of the LSPR shift can be observed in Figure 2d. The results of this characterization are summarized in Figure 2e where the LSPR shift is plotted as a function of DENV2-NS1 protein concentration. The fact that the LSPR shift is technically zero for the control solution validates the effect of the aluminum oxide passivating layer that prevents SU-8 swelling when exposed to aqueous solution for the 10 min period. This small LSPR shift for 0.1 μg/mL concentration (0.038 $\pm$ 0.035 nm) is statistically significant different from the control sample ($p < 0.001$), which suggests the limit of detection in this range. This demonstration shows a promising performance and paves the path for detection of DENV2-NS1 from real biological samples containing elevated concentration of proteins.

In order to assess the device performance in artificial sample conditions, that is, saline solution with high protein content (BSA) and the target biomarker, we repeated the same experiment but we added 100 μg/mL of BSA into the PBS buffer. Figure 2f summarizes the LSPR shift with respect to DENV2-NS1 protein. It is observed that the control solution, PBS+BSA only, has a small background (0.090 $\pm$ 0.024 nm) such as that seen during the surface passivation test, see Figure 2b. However, the LSPR shift as a function of DENV-NS1 protein concentration varies in as much the same way than the case without BSA with sensor response of (0.150 $\pm$ 0.035 nm) for the smallest DENV2-NS1 concentration, which is statistically significant different to the control ($p < 0.001$). Such a demonstration confirms that this biosensing strategy has the potential to detect the target biomarker even in environments where other nonspecific biomolecule binding, BSA in this case, could mask the response. The commercial ssDNA aptamer used in this work was designed against DENV2-NS1. Figure 3 shows the LSPR response from four PBS+BSA (100 μg/mL) solutions containing 10 μg/mL of DENV1-NS1, 10 μg/mL of DENV2-NS1, a mix of 10 μg/mL of each, and control (100 μg/mL of BSA in PBS). DENV2-NS1 protein shares 71.46% of its genomic diversity with DENV1-NS1 protein which can be observed in the finite LSPR response in Figure 3. This limitation prevents intragenotypic DENV identification. In addition, the finite 23% genome similarity with other members of the Flaviviridae virus family adds further selectivity constraints. It is envisioned that further aptamer optimization guided by the unique NS1 genetic code would allow the detection of different DENV genera and others *Flaviviridae* with higher specificity.[32]

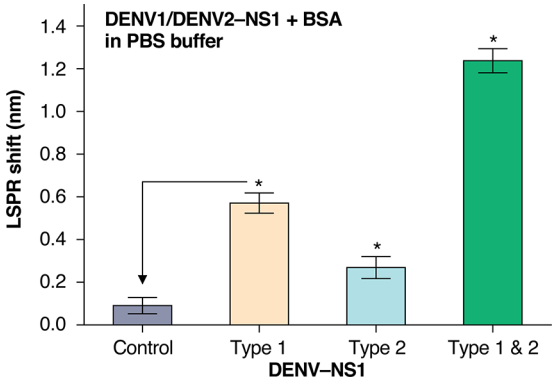

Figure 3. Detection of DENV1 and DENV2 NS1 proteins in PBS. The close genetic match of the NS1 protein between the DENV1 and DENV2 (71.67%) leads to finite LSPR shift when testing DENV1 and DENV2 separate or DENV1+DENV2 combined. Error bars are the standard deviation from the mean. *Unpaired t test and one-way ANOVA with Tukey pairwise comparison ($p < 0.001$).

https://doi.org/10.1021/acs.nanolett.1c01609
Nano Lett. XXXX, XXX, XXX−XXX

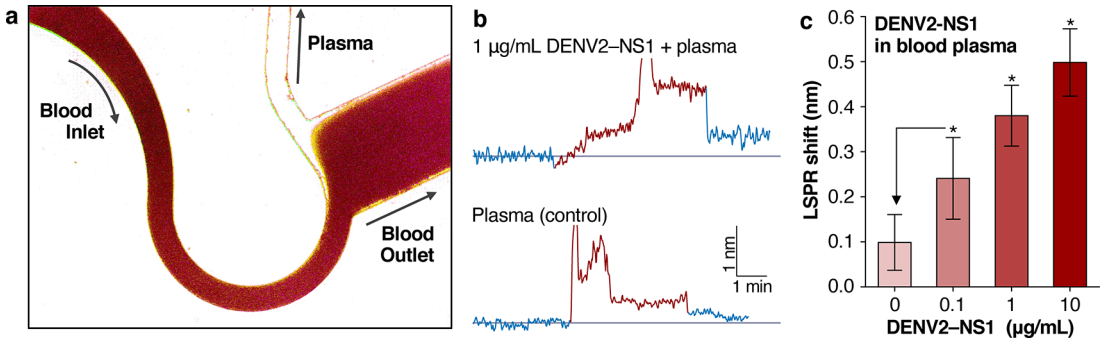

Figure 4. (a) Microscope photograph of blood plasma separation during operation. (b) Two representative sensorgrams during the biosensing demonstration from blood. First a baseline is established by flowing PBS first, then plasma separation is started followed by an incubation time (typ. 3 min) and finalized with PBS flush. (c) DENV2-NS1 protein detection at different concentration (0.1, 1, and 10 μg/mL) in blood and one control (just blood). This biosensing strategy demonstrates biomarker detection from complex biological fluids such as blood plasma. Error bars are the standard deviation from the mean. *Unpaired t test and one-way ANOVA with Tukey pairwise comparison ($p < 0.001$).

Ultimately, a biosensor capable of performing biomarker detection from minimally prepared blood samples is the key for the point-of-care clinical diagnostics and other applications that require portability. In order to demonstrate the feasibility of performing DENV2 detection using the circulating NS1 protein biomarker directly from bovine blood, we integrated the plasmonic biosensor with an on-chip microfluidic plasma separator,[18] see Figure 1a and Methods in the Supporting Information for details. This microfluidic chip uses a combination of biophysical and hydrodynamical effects to generate a cell-free region and extract blood plasma. First, the combination of inertial focusing and Fahraeus effect, implemented in contracting microfluidic bend, imposes lift and drag forces on red/white blood cells and platelets (BCs) directed toward the center of 300 μm or smaller microfluidic channels forming cell-free regions on the walls of the channel termination. Then, bifurcated channels with asymmetric flow rate ratios of at least 2.5:1[33] deviate BCs toward the low resistance path and collects cell-free plasma on the opposite branch.[34−36] Bovine whole blood (~35% hematocrit [hct]) was prepared by spiking a deterministic concentration of DENV2-NS1 protein (0.1, 1, and 10 μg/mL) and control in PBS solution which produced blood samples with ~22.3% hct. Blood samples with lower hct perform better than high htc content blood samples using these type of devices, especially in the low flow regime preventing the noncovalent bonded microfluidic chip from delamination.[34]

Detection directly from blood following this scheme requires four steps. In the first step, PBS and blood flows simultaneously at low speed (~0.02 mL/min) to fill the channels with solution. Once the LSPR signal is stabilized, the PBS channel closes; meanwhile the blood flow increases to ~0.1 mL/min until plasma separation occurs within the first 2 min, see Figure 4a. Once cell-free plasma flows on the active sensing region, the blood flow is stopped and kept off for another 3 min to incubate the plasma sample. Then the PBS channels are open to flush the plasma and other proteins off the active region. Figure 4b shows two LSPR chronograms in which the blue regions are the PBS flow events and the red region correspond to the plasma separation and detection. Spikes in the LSPR are observed mainly due to an event related to the remnant blood cells, refractive index gradients, loss of LSPR tracking, or the reflectance spectra flattening but not biomarker binding. However, flushing with PBS solution allows for the reflectance spectra to recover to the baseline state but with an LSPR shift gained by the binding of the biomarker. As expected, the control sample produces a small background in the same range as in the previous biosensing experiment (0.099 ± 0.024 nm). Nevertheless, DENV2-NS1 protein was clearly differentiated at different concentrations, see Figure 4c. In addition, a similar limit of detection is observed (0.1 μg/mL), where the sensor response is statistically significant, different than the control ($p < 0.001$) and still within the clinical threshold for high risk of DHF development (0.6 μg/mL).

Other methods for DENV detection mostly use immunoassay approaches with the use of antibodies as the affinity layer. For example, the detection of DENV E-protein (see Figure 1b) in the buffer,[37] Immunoglobulin M, as the immune system response to DENV infection, in diluted human serum,[38] and NS1 protein in diluted human blood plasma[39] were performed using the surface plasmon resonance (SPR) method with detection limits in the femtomolar range for DENV E-protein in buffer.[37] Other optical methods such as the luminescence of quantum dots conjugated with the gold nanoparticle via ssDNA aptamers detect purified DENV DNA complementary strands at femtomolar concentrations in the buffer.[40] The flexibility of ssDNA aptamer synthesis combined with the facile surface functionalization strategy enabled the detection of other virus biomarkers using SPR[41,42] or electrochemical techniques.[43−45] Unlike other demonstrations, this work shows the use of a hybrid microfluidic−plasmonic device as a promising technique for the rapid sample preparation (plasma separation) and antigen detection with comparable detection ranges as other SPR based sensors. This work represents an attractive approach for the detection of viruses directly from blood with comparable assay time (<10 min) and clinically relevant limit of detection (0.1 μg/mL).

Success in containing the spread of viral infections relies on the early and accurate detection of biomarkers in biological fluids, ideally in the infection stages prior to the onset of life-threatening symptoms. In addition, as several viral infections manifest as similar symptoms at the early stages, and most of them can develop into chronic pathologies, any misdiagnosis can lead to severe medical complications leading to death. In this context, the work presented here demonstrated a biosensing platform with potential portability for deploying to the sites of interest, for example, in remote locations lacking the adequate infrastructure for prompt screening. Nanoimprint lithography offers parallel, low-cost and high throughput

https://doi.org/10.1021/acs.nanolett.1c01609
Nano Lett. XXXX, XXX, XXX−XXX

nanopatterning capabilities that, when combined with industrial batch processing, paves the path for commercialization. It is envisaged that with further sensor optimization, multiplexing, and hardware/software integration this platform can become a practical solution to detect a myriad of other biomarkers, not only the different genera from the *Flaviviridae* virus family but to other relevant pathologies associated with viral infections, such as the current COVID-19 pandemic caused by the SARS-CoV-2 virus.

■ ASSOCIATED CONTENT

Supporting Information

The Supporting Information is available free of charge at https://pubs.acs.org/doi/10.1021/acs.nanolett.1c01609.

Detailed information about the device fabrication, optical simulations, device characterization, sensor functionalization, and sensor characterizations (PDF)

■ AUTHOR INFORMATION

Corresponding Author

Debashis Chanda − *CREOL, The College of Optics and Photonics and Department of Physics, University of Central Florida, Orlando, Florida 32816, United States; NanoScience Technology Center, University of Central Florida, Orlando, Florida 32826, United States*; Email: debashis.chanda@ucf.edu

Authors

Abraham Vázquez-Guardado − *CREOL, The College of Optics and Photonics, University of Central Florida, Orlando, Florida 32816, United States; NanoScience Technology Center, University of Central Florida, Orlando, Florida 32826, United States*; orcid.org/0000-0002-0648-5921

Freya Mehta − *Burnett School of Biomedical Sciences, College of Medicine, University of Central Florida, Orlando, Florida 32816, United States*

Beatriz Jimenez − *Department of Electrical and Computer Engineering, University of Central Florida, Orlando, Florida 32816, United States*

Aritra Biswas − *CREOL, The College of Optics and Photonics, University of Central Florida, Orlando, Florida 32816, United States; NanoScience Technology Center, University of Central Florida, Orlando, Florida 32826, United States*

Keval Ray − *Burnett School of Biomedical Sciences, College of Medicine, University of Central Florida, Orlando, Florida 32816, United States*

Aliyah Baksh − *NanoScience Technology Center, University of Central Florida, Orlando, Florida 32826, United States*

Sang Lee − *NanoScience Technology Center, University of Central Florida, Orlando, Florida 32826, United States*

Nileshi Saraf − *Materials Science and Engineering, Advanced Materials Processing and Analysis Center, University of Central Florida, Orlando, Florida 32816, United States*

Sudipta Seal − *NanoScience Technology Center, University of Central Florida, Orlando, Florida 32826, United States; Materials Science and Engineering, Advanced Materials Processing and Analysis Center, University of Central Florida, Orlando, Florida 32816, United States; College of Medicine, University of Central Florida, Orlando, Florida 32827, United States*; orcid.org/0000-0002-0963-3344

Complete contact information is available at: https://pubs.acs.org/10.1021/acs.nanolett.1c01609

Author Contributions

A.V.G. and D.C. conceptualized the idea. A.V.G., F.M., B.J., A.B., K.R., A.B., S.L., and N.S. performed the experiments. F.M., A.B., and K.R. prepared the biological samples. A.B. fabricated the sensors and performed the numerical simulations. A.V.G. designed the experiments and analyzed the data. D.C. and S.S. contributed with materials and reagents. A.V.G. and D.C. wrote the manuscript and other authors contributed and edited the manuscript.

Notes

The authors declare no competing financial interest.

■ ACKNOWLEDGMENTS

This work at University of Central Florida was partially supported by National Science Foundation under Grant ECCS-1808045 and UCF COVID-19 Artificial Intelligence and Big Data (AI & BD) Initiative Seed Funding Program 2020-2021. B.J. acknowledges the National Science Foundation for support of this work through the REU site EEC 1560007.

■ REFERENCES

(1) Rodriguez-Roche, R.; Gould, E. A. Understanding the Dengue Viruses and Progress towards Their Control. *BioMed Res. Int.* **2013**, *2013*, 1−20.

(2) Guzman, M. G.; Halstead, S. B.; Artsob, H.; Buchy, P.; Farrar, J.; Gubler, D. J.; Hunsperger, E.; Kroeger, A.; Margolis, H. S.; Martínez, E.; Nathan, M. B.; Pelegrino, J. L.; Simmons, C.; Yoksan, S.; Peeling, R. W. Dengue: A Continuing Global Threat. *Nat. Rev. Microbiol.* **2010**, *8* (S12), S7−S16.

(3) Tuiskunen Bäck, A.; Lundkvist, Å. Dengue Viruses − an Overview. *Infect. Ecol. Epidemiol.* **2013**, *3* (1), 19839.

(4) Yung, C. F.; Lee, K. S.; Thein, T. L.; Tan, L. K.; Gan, V. C.; Wong, J. G. X.; Lye, D. C.; Ng, L. C.; Leo, Y. S. Dengue Serotype-Specific Differences in Clinical Manifestation, Laboratory Parameters and Risk of Severe Disease in Adults, Singapore. *Am. J. Trop. Med. Hyg.* **2015**, *92* (5), 999−1005.

(5) Whitehorn, J.; Simmons, C. P. The Pathogenesis of Dengue. *Vaccine* **2011**, *29* (42), 7221−7228.

(6) Coller, B.-A. G.; Clements, D. E. Dengue Vaccines: Progress and Challenges. *Curr. Opin. Immunol.* **2011**, *23* (3), 391−398.

(7) Chokephaibulkit, K.; Perng, G. C. Challenges for the Formulation of a Universal Vaccine against Dengue. *Exp. Biol. Med.* **2013**, *238* (5), 566−578.

(8) Rosa, B. R.; Cunha, A. J. L. A. Da; Medronho, R. D. A. Efficacy, Immunogenicity and Safety of a Recombinant Tetravalent Dengue Vaccine (CYD-TDV) in Children Aged 2−17 Years: Systematic Review and Meta-Analysis. *BMJ. Open* **2019**, *9* (3), e019368.

(9) World Health Organization. *Dengue Vaccine Safety Update*; World Health Organization, 2017. Available at https://www.who.int/groups/global-advisory-committee-on-vaccine-safety/topics/dengue-vaccines/safety-update/ (accessed 2021-08-23).

(10) Vázquez, S.; Lemos, G.; Pupo, M.; Ganzón, O.; Palenzuela, D.; Indart, A.; Guzmán, M. G. Diagnosis of Dengue Virus Infection by the Visual and Simple AuBioDOT Immunoglobulin M Capture System. *Clin. Vaccine Immunol.* **2003**, *10* (6), 1074−1077.

(11) Alcon, S.; Talarmin, A.; Debruyne, M.; Falconar, A.; Deubel, V.; Flamand, M. Enzyme-Linked Immunosorbent Assay Specific to Dengue Virus Type 1 Nonstructural Protein NS1 Reveals Circulation of the Antigen in the Blood during the Acute Phase of Disease in Patients Experiencing Primary or Secondary Infections. *J. Clin. Microbiol.* **2002**, *40* (2), 376−381.

(12) Sa-Ngasang, A.; Wibulwattanakij, S.; Chanama, S.; O-Rapinpatipat, A.; A-Nuegoonpipat, A.; Anantapreecha, S.; Sawanpanyalert, P.; Kurane, I. Evaluation of RT-PCR as a Tool for

Diagnosis of Secondary Dengue Virus Infection. *Jpn. J. Infect. Dis.* **2003**, *56* (5−6), 205−209.
(13) Lolekha, R.; Chokephaibulkit, K.; Yoksan, S.; Vanprapar, N.; Phongsamart, W.; Chearskul, S. Diagnosis of Dengue Infection Using Various Diagnostic Tests in the Early Stage of Illness. *Southeast Asian J. Trop. Med. Public Health* **2004**, *35* (2), 391−395.
(14) Sharma, S.; Kumari, R.; Varshney, S. K.; Lahiri, B. Optical Biosensing with Electromagnetic Nanostructures. *Rev. Phys.* **2020**, *5*, 100044.
(15) Yang, T.; Chen, S.; He, X.; Guo, H.; Sun, X. How to Convincingly Measure Low Concentration Samples with Optical Label-Free Biosensors. *Sens. Actuators, B* **2020**, *306*, 127568.
(16) Chanda, D.; Shigeta, K.; Truong, T.; Lui, E.; Mihi, A.; Schulmerich, M.; Braun, P. V.; Bhargava, R.; Rogers, J. A. Coupling of Plasmonic and Optical Cavity Modes in Quasi-Three-Dimensional Plasmonic Crystals. *Nat. Commun.* **2011**, *2* (1), 479.
(17) Vázquez-Guardado, A.; Smith, A.; Wilson, W.; Ortega, J.; Perez, J. M.; Chanda, D. Hybrid Cavity-Coupled Plasmonic Biosensors for Low Concentration, Label-Free and Selective Biomolecular Detection. *Opt. Express* **2016**, *24* (22), 25785.
(18) Vázquez-Guardado, A.; Barkam, S.; Peppler, M.; Biswas, A.; Dennis, W.; Das, S.; Seal, S.; Chanda, D. Enzyme-Free Plasmonic Biosensor for Direct Detection of Neurotransmitter Dopamine from Whole Blood. *Nano Lett.* **2019**, *19* (1), 449.
(19) Vázquez-Guardado, A.; Safaei, A.; Modak, S.; Franklin, D.; Chanda, D. Hybrid Coupling Mechanism in a System Supporting High Order Diffraction, Plasmonic, and Cavity Resonances. *Phys. Rev. Lett.* **2014**, *113* (26), 263902 DOI: 10.1103/PhysRevLett.113.263902.
(20) Libraty, D. H.; Young, P. R.; Pickering, D.; Endy, T. P.; Kalayanarooj, S.; Green, S.; Vaughn, D. W.; Nisalak, A.; Ennis, F. A.; Rothman, A. L. High Circulating Levels of the Dengue Virus Nonstructural Protein NS1 Early in Dengue Illness Correlate with the Development of Dengue Hemorrhagic Fever. *J. Infect. Dis.* **2002**, *186* (8), 1165−1168.
(21) Ameling, R.; Langguth, L.; Hentschel, M.; Mesch, M.; Braun, P. V.; Giessen, H. Cavity-Enhanced Localized Plasmon Resonance Sensing. *Appl. Phys. Lett.* **2010**, *97* (25), 253116.
(22) Wouters, K.; Puers, R. Diffusing and Swelling in SU-8: Insight in Material Properties and Processing. *J. Micromech. Microeng.* **2010**, *20* (9), No. 095013.
(23) Young, L. B.; Melian, E. B.; Setoh, Y. X.; Young, P. R.; Khromykh, A. A. Last 20 Aa of the West Nile Virus NS1 Protein Are Responsible for Its Retention in Cells and the Formation of Unique Heat-Stable Dimers. *J. Gen. Virol.* **2015**, *96* (5), 1042−1054.
(24) Bailey, M. J.; Duehr, J.; Dulin, H.; Broecker, F.; Brown, J. A.; Arumemi, F. O.; Bermúdez González, M. C.; Leyva-Grado, V. H.; Evans, M. J.; Simon, V.; Lim, J. K.; Krammer, F.; Hai, R.; Palese, P.; Tan, G. S. Human Antibodies Targeting Zika Virus NS1 Provide Protection against Disease in a Mouse Model. *Nat. Commun.* **2018**, *9* (1), 1−11.
(25) Rastogi, M.; Sharma, N.; Singh, S. K. Flavivirus NS1: A Multifaceted Enigmatic Viral Protein. *Virol. J.* **2016**, *13* (1), 1−10.
(26) Madeira, F.; Park, Y. mi; Lee, J.; Buso, N.; Gur, T.; Madhusoodanan, N.; Basutkar, P.; Tivey, A. R. N.; Potter, S. C.; Finn, R. D.; Lopez, R. The EMBL-EBI Search and Sequence Analysis Tools APIs in 2019. *Nucleic Acids Res.* **2019**, *47* (W1), W636−W641.
(27) Gutsche, I.; Coulibaly, F.; Voss, J. E.; Salmon, J.; D'Alayer, J.; Ermonval, M.; Larquet, E.; Charneau, P.; Krey, T.; Megret, F.; Guittet, E.; Rey, F. A.; Flamand, M. Secreted Dengue Virus Nonstructural Protein NS1 Is an Atypical Barrel-Shaped High-Density Lipoprotein. *Proc. Natl. Acad. Sci. U. S. A.* **2011**, *108* (19), 8003−8008.
(28) Flamand, M.; Megret, F.; Mathieu, M.; Lepault, J.; Rey, F. A.; Deubel, V. Dengue Virus Type 1 Nonstructural Glycoprotein NS1 Is Secreted from Mammalian Cells as a Soluble Hexamer in a Glycosylation-Dependent Fashion. *J. Virol.* **1999**, *73* (7), 6104−6110.
(29) Arroyo-Currás, N.; Somerson, J.; Vieira, P. A.; Ploense, K. L.; Kippin, T. E.; Plaxco, K. W. Real-Time Measurement of Small Molecules Directly in Awake, Ambulatory Animals. *Proc. Natl. Acad. Sci. U. S. A.* **2017**, *114* (4), 645−650.
(30) Herne, T. M.; Tarlov, M. J. Characterization of DNA Probes Immobilized on Gold Surfaces. *J. Am. Chem. Soc.* **1997**, *119* (38), 8916−8920.
(31) Dykstra, P. H.; Roy, V.; Byrd, C.; Bentley, W. E.; Ghodssi, R. Microfluidic Electrochemical Sensor Array for Characterizing Protein Interactions with Various Functionalized Surfaces. *Anal. Chem.* **2011**, *83* (15), 5920−5927.
(32) Chang, H.-H.; Huber, R. G.; Bond, P. J.; Grad, Y. H.; Camerini, D.; Maurer-Stroh, S.; Lipsitch, M. Systematic Analysis of Protein Identity between Zika Virus and Other Arthropod-Borne Viruses. *Bull. World Health Organ.* **2017**, *95* (7), 517−525I.
(33) Yang, S.; Ündar, A.; Zahn, J. D. A Microfluidic Device for Continuous, Real Time Blood Plasma Separation. *Lab Chip* **2006**, *6* (7), 871−880.
(34) Tripathi, S.; Kumar, Y. V. B.; Agrawal, A.; Prabhakar, A.; Joshi, S. S. Microdevice for Plasma Separation from Whole Human Blood Using Bio-Physical and Geometrical Effects. *Sci. Rep.* **2016**, *6* (1), 26749.
(35) Martel, J. M.; Toner, M. Particle Focusing in Curved Microfluidic Channels. *Sci. Rep.* **2013**, *3* (1), 3340.
(36) Di Carlo, D.; Edd, J. F.; Irimia, D.; Tompkins, R. G.; Toner, M. Equilibrium Separation and Filtration of Particles Using Differential Inertial Focusing. *Anal. Chem.* **2008**, *80* (6), 2204−2211.
(37) Omar, N. A. S.; Fen, Y. W.; Abdullah, J.; Mustapha Kamil, Y.; Daniyal, W. M. E. M. M.; Sadrolhosseini, A. R.; Mahdi, M. A. Sensitive Detection of Dengue Virus Type 2 E-Proteins Signals Using Self-Assembled Monolayers/Reduced Graphene Oxide-PAMAM Dendrimer Thin Film-SPR Optical Sensor. *Sci. Rep.* **2020**, *10* (1), 2374.
(38) Jahanshahi, P.; Zalnezhad, E.; Sekaran, S. D.; Adikan, F. R. M. Rapid Immunoglobulin M-Based Dengue Diagnostic Test Using Surface Plasmon Resonance Biosensor. *Sci. Rep.* **2015**, *4* (1), 3851.
(39) Wong, W. R.; Sekaran, S. D.; Mahamd Adikan, F. R.; Berini, P. Detection of Dengue NS1 Antigen Using Long-Range Surface Plasmon Waveguides. *Biosens. Bioelectron.* **2016**, *78*, 132−139.
(40) Chowdhury, A. D.; Takemura, K.; Khorish, I. M.; Nasrin, F.; Ngwe Tun, M. M.; Morita, K.; Park, E. Y. The Detection and Identification of Dengue Virus Serotypes with Quantum Dot and AuNP Regulated Localized Surface Plasmon Resonance. *Nanoscale Adv.* **2020**, *2* (2), 699−709.
(41) Lautner, G.; Balogh, Z.; Bardóczy, V.; Mészáros, T.; Gyurcsányi, R. E. Aptamer-Based Biochips for Label-Free Detection of Plant Virus Coat Proteins by SPR Imaging. *Analyst* **2010**, *135* (5), 918.
(42) Shrivastav, A. M.; Cvelbar, U.; Abdulhalim, I. A Comprehensive Review on Plasmonic-Based Biosensors Used in Viral Diagnostics. *Commun. Biol.* **2021**, *4* (1), 70.
(43) Bartosik, M.; Durikova, H.; Vojtesek, B.; Anton, M.; Jandakova, E.; Hrstka, R. Electrochemical Chip-Based Genomagnetic Assay for Detection of High-Risk Human Papillomavirus DNA. *Biosens. Bioelectron.* **2016**, *83*, 300−305.
(44) Lum, J.; Wang, R.; Hargis, B.; Tung, S.; Bottje, W.; Lu, H.; Li, Y. An Impedance Aptasensor with Microfluidic Chips for Specific Detection of H5N1 Avian Influenza Virus. *Sensors* **2015**, *15* (8), 18565−18578.
(45) Saraf, N.; Villegas, M.; Willenberg, B. J.; Seal, S. Multiplex Viral Detection Platform Based on a Aptamers-Integrated Microfluidic Channel. *ACS Omega* **2019**, *4* (1), 2234−2240.

https://doi.org/10.1021/acs.nanolett.1c01609
Nano Lett. XXXX, XXX, XXX−XXX